

A COMPUTATIONAL METHOD FOR OPTIMIZING STORAGE PLACEMENT TO MAXIMIZE POWER NETWORK RELIABILITY

Debarati Bhaumik
Daan Crommelin
Bert Zwart

CWI Amsterdam
Science Park 123
Amsterdam, 1098 XG, NETHERLANDS

ABSTRACT

The intermittent nature of renewable energy sources challenges the power network reliability. However, these challenges can be alleviated by incorporating energy storage devices into the network. We develop a computational technique which can find the optimal storage placement in the network with stochastic power injections, subject to minimizing a reliability index: the *probability of a line current violation*. We use the *simulated annealing* algorithm to minimize this probability under the variation of storage locations and capacities in the network, keeping the total storage capacity constant. In order to estimate the small probabilities of line current violations we use the *splitting technique* of rare-event simulation. We construct an appropriate *importance function* for splitting which enhances the efficiency of the probability estimator compared to the conventional Crude Monte Carlo estimator. As an illustration, we apply our method to the IEEE-14 bus network.

1 INTRODUCTION

The strive for reducing carbon footprints and a carbon free future has rapidly increased the usage of renewable energies in power networks. Renewable energy sources like photo-voltaic (PV) arrays and wind turbines are unpredictable in nature, which lead to intermittent power generation. The integration of intermittent renewable energy sources into the electrical power network challenges the network reliability.

However, network reliability can be enhanced by incorporating energy storage devices (batteries) in the network. The energy storage device acts as buffer by storing excess energy generated and delivering power when there is energy deficiency. The peak-shaving benefit of batteries have been studied long back in 1981 by Yau, Walker, Graham, Gupta, and Raithel (1981). Barton and Infield (2004) developed a probabilistic method to study the ability of energy storage to increase penetration of intermittent energy sources in power grids.

Recent studies have investigated storage placement in the power network under the framework of optimal power flow in Varaiya, Wu, and Bialek (2011), Ghofrani, Arabali, Etezadi-Amoli, and Fadali (2013), Gayme and Topcu (2013), Sjödin, Gayme, and Topcu (2012), Aburub and Jewell (2014), Bose, Gayme, Topcu, and Chandy (2012), Oh (2011) and Chandy, Low, Topcu, and Xu (2010). Ghofrani, Arabali, Etezadi-Amoli, and Fadali (2013) minimized the hourly social cost using a market-based probabilistic optimal power flow with energy storage integration and wind generation. Gayme and Topcu (2013) proposed a solution strategy to solve the optimal control problem to investigate the effects of different energy storage capacities on generation costs and peak-shaving. However, they have neglected uncertainties due to fluctuations in demand and intermittency in generation. To study the energy storage dispatch and placement problem in power network with wind generation, Sjödin, Gayme, and Topcu (2012) proposed a risk-mitigated optimal

power flow framework. Bose, Gayme, Topcu, and Chandy (2012) studied optimal placement of large-scale energy storage in power grids using semidefinite relaxation of AC optimal power flow. Oh (2011) proposed a method to model the storage devices under the framework of DC optimal power flow.

This study focuses on the optimal storage placement in a power network for reliable operation of the network. We model the line currents in the network according to the DC power flow equations and consider the Probability of Line Current Violation (PLCV) as the *reliability index* of the network. PLCV calculates the probability that one of the lines in the network has been overloaded, i.e., one of the line currents has exceeded its allowed maximum. These line current violations lead to physical damage to the lines because of the eventual temperature overload.

Given the distribution of the stochastic processes of the uncertain power injections and the total storage installation size, we aim to find the optimal placement of the storage devices in the network such that the PLCV is minimal. In order to do so, we use the *Simulated Annealing* algorithm to minimize the PLCV in the configuration space of different storage sizes and locations. We resort to simulated annealing because the configuration space of different storage locations and capacities is very large and the quantity we wish to minimize (the PLCV) is not guaranteed to be convex. van den Akker, Leemhuis, and Bloemhof (2014) have briefly discussed using simulated annealing for optimal storage placement in power network to minimize generation cost. Our study focuses on minimizing a cost function which is a rare-event probability.

For reliable operation of power network, PLCV should be small. The conventional Crude Monte Carlo (CMC) method is robust but becomes very inefficient for estimating small probabilities. To increase the efficiency we use the *Splitting Technique* for rare-event simulations (Rubino, Tuffin, et al. 2009). We use a variant of splitting called the Fixed Number of Successes (FNS) proposed by Amrein and Künsch (2011). Wadman, Crommelin, and Frank (2013) used FNS to estimate electrical grid reliability. The efficiency of splitting is highly dependent on the *Importance Function* used (Garvels, Van Ommeren, and Kroese 2002). We develop an appropriate IF for our problem. We verify numerically that our IF works well. A theoretical analysis would be interesting but is beyond the scope of the paper. Note that this is non-trivial since the power injections in the networks are not diffusion processes due to the buffers (storage devices), and as such, our setting does not fit in the framework of Wadman, Crommelin, and Zwart (2016).

To the best of our knowledge, the combination of rare-event simulation with simulated annealing has not been carried out before. Shortle, Rebennack, and Glover (2014) used splitting to estimate the probability of large-scale blackout in power network, which is embedded within a higher level optimization technique to minimize the probability subjected to a budget constraint. We apply our method to the IEEE-14 bus test case network. The uncertain power injections are modeled as Ornstein-Uhlenbeck processes. Given a fixed total storage instalment capacity, we find the optimal storage locations and capacities at each nodes of the network such that the PLCV is minimal. The total fixed storage installation capacity reflects financial/physical constraints. We start from different initial configurations of the storage locations and capacities to check the convergence of simulated annealing to the final storage configuration.

In section 2 we discuss the DC power flow equations and the stochastic processes used to model the net power generation and the storage model. Section 3 defines the problem. Section 4 introduces simulated annealing algorithm and its various aspects used in the problem. Section 5 provides details of the FNS splitting technique and the IF used for the problem. Section 6 presents the simulation results showing how SA algorithm along with FNS minimizes PLCV efficiently for the given IEEE-14 bus test case network. Finally we conclude in section 7.

2 SYSTEM SET UP

Let the power network be modeled by a graph $\mathcal{G} = (\mathcal{N}, \mathcal{E})$, where $\mathcal{N} := \{1, 2, \dots, N\}$ is the set of nodes (also called buses) and \mathcal{E} is the set of edges (also called lines). We solve the DC power flow equations for calculating the line currents.

2.1 DC Power Flow Equations

The standard AC power flow equations are non-linear (Grainger and Stevenson 1994). A common linear approximation of the AC power flow equation (Grainger and Stevenson 1994) leads to the so-called DC power flow equations

$$P_i = \sum_{j=1}^N B_{i,j}(\theta_i - \theta_j) \quad (i \in \mathcal{N}), \quad (1)$$

where P_i is the net real power injection at node i , θ_i is the voltage phase angle at bus i and $B_{i,j} = B_{j,i}$ is the susceptance of the line connection $(i, j) \in \mathcal{E}$. For any line $(i, j) \in \mathcal{E}$, the line current $I_{i,j}$ flowing from $i \rightarrow j$ is given by Ohm's Law, i.e., $I_{i,j} = B_{i,j}(\theta_i - \theta_j)$.

For the slack bus 1, we set $\theta_1 = 0$ and $P_1 = -\sum_{j=2}^N P_j$. The slack bus is the only bus for which the system reference voltage angle is defined. It also balances the net power injection in the system.

2.2 Power Generation

We interpret every non-slack node as a single household which has stochastic generation $G(t)$ and demand $D(t)$ at time t and produces net power $P(t) := G(t) - D(t)$. We model the net power generation at the i -th non-slack node $P_i(t)$ as discretized Ornstein-Uhlenbeck (O-U) processes which are in fact AR(1) processes,

$$\Delta P_i(t) = \beta_i(\mu_i - P_i(t))\Delta t + \sigma_i \Delta W_i(t) \text{ for } i = 1, \dots, N-1. \quad (2)$$

where μ_i is the long term mean, β_i is the mean reverting term, σ_i is the volatility term and $W_i(t)$ denotes the Wiener process of the i^{th} O-U process. The values of these terms are determined later in section 6. Modelling power injections as O-U processes have been suggested by Wadman, Crommelin, and Frank (2013) and Wadman, Crommelin, and Zwart (2016).

2.3 Storage Model

We consider the storage devices (batteries) to be co-located with the stochastic non-slack nodes and are charged/discharged locally by the net power produced at each node. Let $B_i(t)$ be the level of energy stored in the battery at time t at the i -th non-slack node, and it has a maximum capacity B_i^{\max} . The batteries are updated according to

$$B_i(t + \Delta t) = B_i(t) + p_i^{\text{B}}(t)\Delta t \quad \forall t \in [0, T], \quad (3)$$

where $p_i^{\text{B}}(t)$ is the power flowing in/out of i -th the battery, Δt is the length of the time step and T is the time horizon of interest. The batteries are bounded by their corresponding capacity and total installation capacity constraints

$$0 \leq B_i(t) \leq B_i^{\max} \quad \text{and} \quad \sum_i B_i^{\max} = B^{\text{tot}} \quad \forall t \in [0, T]. \quad (4)$$

Let $P_i^{\text{B}}(t)$ be the power generated by the i -th battery and is given by $P_i^{\text{B}}(t) = -p_i^{\text{B}}(t)$. This is because, $p_i^{\text{B}}(t) > 0$ implies the battery is getting charged and it is consuming power and $p_i^{\text{B}}(t) < 0$ implies the battery is discharging and is generating power.

2.3.1 Switching of the Battery

The battery charging/discharging depends on the power flowing in/out of the battery $p_i^{\text{B}}(t)$ which is given by

$$p_i^{\text{B}}(t) = \begin{cases} P_i(t) & \text{if } 0 \leq X_i(t) \leq B_i^{\max} \\ (B_i^{\max} - B_i(t))/\Delta t & \text{if } X_i(t) > B_i^{\max} \\ -B_i(t)/\Delta t & \text{if } X_i(t) < 0. \end{cases} \quad (5)$$

where $X_i(t) = P_i(t)\Delta t + B_i(t)$ for $i = 1, \dots, N - 1$. $X_i(t)$ is the energy level of the battery at time t without any constraints imposed. Hence the battery charging/discharging is dependent on the net power generated by the stochastic non-slack buses and the state of the battery. The above equation (5) ensures that (4) is true. To keep the storage model simple we neglect the *ramp constraints*, the imposed maximal charging/discharging rate on the storage device in this study.

3 PROBLEM DESCRIPTION

Our aim is to find the optimal battery locations and capacities at each node to ensure a reliable operation of the network. We consider the *Probability of Line Current Violation* (PLCV) as the reliability index of the network. PLCV is defined as the probability that any one of the line currents violate its given line constraint maximum at any time $t \in [0, T]$, i.e,

$$\gamma := \mathcal{P}\{\exists(i, j) \in \mathcal{E} : \sup_{t \in [0, T]} |I_{i,j}(t)| \geq I_{i,j}^{\max}\}. \quad (6)$$

In the above equation $I_{i,j}$ is the current flowing between nodes i and j and $I_{i,j}^{\max} > 0$ is the maximum current carrying capacity the edge connecting nodes i and j .

To solve the optimal storage (battery) placement problem and calculating PLCV we use a novel combination of two algorithms namely the *simulated annealing* algorithm and the *splitting* technique for rare-event simulations, respectively, discussed in the subsequent sections.

4 SIMULATED ANNEALING (SA) ALGORITHM

We wish to find the optimal location and capacities of the battery in the network such that PLCV is minimal. We do not expect PLCV to be convex. Also, the configuration of space of battery locations and capacities to grow exponentially with the number of nodes in the network. To overcome these problems we use the Simulated Annealing (SA) (Van Laarhoven and Aarts 1987) algorithm to minimize PLCV.

Simulated annealing is a metaheuristic algorithm designed to approximate the global optimum of a given function. The main aim of the algorithm is to perform a local search in the solution space \mathbf{X} of the problem to minimize a desired *cost function* $f(\mathbf{X})$. Annealing is a physical process of heating a solid to very high temperature, then it is cooled by slowly lowering the temperature of the solid for eliminating point defects. It should be noted that there is no hard guarantee to find the global optimum using SA. The SA algorithm is based on the following search principle :

1. Start with an initial solution and consider it as the best solution \mathbf{X}_{best} . Initialize T_c , the temperature of the *acceptance probability* of a *bad* solution .
2. Randomly select a new solution \mathbf{X}^* in the neighbourhood of the previously obtained best solution.
3. If the new solution is better than the previously found best solution, i.e, if $\Delta E = f(\mathbf{X}^*) - f(\mathbf{X}_{\text{best}}) < 0$, then consider the new solution as the best solution $\mathbf{X}_{\text{best}} = \mathbf{X}^*$.
4. If not, i.e, $\Delta E = f(\mathbf{X}^*) - f(\mathbf{X}_{\text{best}}) > 0$, then accept the new *bad* solution as the best solution with a probability $\exp(-\Delta E/T_c)$.
5. Slowly cool the temperature of the acceptance probability (decrease T_c).
6. Repeat from 2 until the *stopping criterion* is reached.

The cooling law has to be chosen carefully to allow the algorithm sufficiently explore the region around the initial guess. If the cooling is too fast, the system will get stuck in the nearest local minimum and the algorithm may not converge. If the cooling is too slow, the algorithm spends a lot of time in useless explorations which slows down the process. Usually, an exponential decrease is considered for the cooling by multiplying the current temperature with a constant, i.e. $T_c^{\text{new}} = \kappa T_c^{\text{old}}$ where $0 < \kappa < 1$.

4.1 Cost Function: $\log(\gamma)$

In this study we want to minimize γ (PLCV (6)) in the battery locations and capacities configuration space. The values of γ 's are typically small and while minimizing can go down to $\sim 10^{-5} - 10^{-7}$ or smaller depending on the total installation capacity of the battery. The *acceptance probability* of the bad solution not only depends on T_c but also on the difference of the function values for the new solution and the previously found best solution $\Delta E = \gamma(\mathbf{X}^*) - \gamma(\mathbf{X}_{\text{best}})$. As the γ 's are very small, their differences are also small hence the acceptance probability becomes large and the algorithm accepts too many bad solutions and might never converge. So, instead of minimizing γ we minimize $\log(\gamma)$ such that $\Delta E = \log(\gamma(\mathbf{X}^*)) - \log(\gamma(\mathbf{X}_{\text{best}}))$ does not take very small values and the algorithm does not accept too many bad solutions.

4.2 Random Moves in Battery Configuration Space

We evaluate γ for different battery locations and capacities in the SA algorithm and then minimize $\log(\gamma)$. To move randomly in the solution configuration space, we randomly select two non-slack nodes $(i, j) \forall i \in \mathcal{N}/\{1\}$ and $\forall j(\neq i) \in \mathcal{N}/\{1\}$. Then exchange m_B blocks of battery unit ΔB between the two chosen nodes such that conditions in (4) are satisfied. Initially we start the algorithm by exchanging $m_B = N_B$ blocks of the battery unit and gradually reduce m_B till it is equal to 1. The gradual reduction of m_B depends on the decrease of γ . As the value of γ reduces by a factor of 10, m_B is decreased by Δm . This ensures that when the desired minimum is reached the system does not jump out of the minimum. The values of ΔB , N_B and Δm will be discussed in subsequent sections.

4.3 Stopping Criterion for SA

We enforce three simultaneous *stopping criteria* for SA algorithm:

1. The number of iterations, n_{iter} , exceeds a pre-defined threshold value, n_{max} , i.e., $n_{\text{iter}} \geq n_{\text{max}}$.
2. The difference between n_{iter} and the number of solutions the algorithm has accepted, n_a , exceeds a maximum value, n_d , i.e., $n_{\text{iter}} - n_a \geq n_d$.
3. The improvements in γ have reached a desired minimum, ε , i.e., $\gamma_{\min} = \max_{n_m} |\gamma^{n_a} - \gamma^{n_a - n_m}| \leq \varepsilon$, where γ^{n_a} is γ for the accepted iteration n_a .

If any of the stopping criteria is true the algorithm stops.

5 FIXED NUMBER OF SUCCESSES SPLITTING TECHNIQUE

In our model we are interested in estimating PLCV and then minimize the logarithm of PLCV. It is expected that PLCV will take very small values during minimization. The Crude Monte Carlo (CMC) estimations of these small probabilities will become computationally very expensive and thus we use the *splitting technique* for rare-event simulations. In this section we give a brief overview of the splitting technique, following Bhaumik, Crommelin, and Zwart (2015) closely.

5.1 Splitting Technique for Rare-Event Simulation

Let $(\Omega, \mathcal{F}, \mathcal{P})$ be a probability space and $R \in \mathcal{F}$ be the rare event set of interest (Rubino, Tuffin, et al. 2009). The probability of reaching the rare-event set R , $\tilde{\gamma} = \mathcal{P}(R)$ will be small. The CMC estimator of $\mathcal{P}(R)$ and the *squared relative error* of the CMC estimator are given by,

$$\tilde{\gamma} := \frac{1}{M} \sum_{j=1}^M \mathbb{1}_{\{\text{sample } j \text{ reaches } R\}} \quad \text{and} \quad \text{SRE}(\tilde{\gamma}) := \frac{\text{Var}(\tilde{\gamma})}{\tilde{\gamma}^2} = \frac{1 - \tilde{\gamma}}{\tilde{\gamma}M}. \quad (7)$$

M is the number of samples generated. CMC probability estimator becomes unreliable for small $\tilde{\gamma}$. This is because, the $\text{SRE}(\tilde{\gamma}) \rightarrow \infty$ as $\tilde{\gamma} \rightarrow 0$ for fixed M . Otherwise to achieve an acceptable SRE we need very

large values of M . For example, to estimate probabilities smaller than 10^{-4} one needs $M \gtrsim 10^6$ CMC samples for achieving $\text{SRE} \approx 0.01$.

The computational workload for estimation small probabilities of rare-events can be reduced by using rare-event simulations techniques like Importance Sampling and Splitting (Rubino, Tuffin, et al. 2009). We use the *splitting* technique for estimating $\tilde{\gamma}$ in our simulations (Garvels 2000). In splitting, the distance to the rare-event set is measured in terms of the *Importance Function* (IF). The sample paths of the stochastic processes involved are split into multiple copies at various levels of the IF till the rare event set is reached. The probability $\tilde{\gamma}$ is decomposed into the product of several conditional probabilities which are non-rare and are hence less computationally intensive to calculate. The most important ingredient of splitting is to find an appropriate IF for the problem.

Let $\mathbf{X}(t) := (X_1(t), \dots, X_n(t))$, $\forall t \geq 0$ be a vector of Markov processes with state space ξ . The importance function, $\phi(\mathbf{X}(t)) : \xi \rightarrow \mathbb{R}$, assigns importance values to $\mathbf{X}(t)$. Let $R_{\phi,L,t} = \{\mathbf{X}(t) \in \xi : \phi(\mathbf{X}(t)) \geq L\}$ be the rare event set defined in terms of ϕ . We are interested in the rare event $R = \{\exists t \leq T : R_{\phi,L,t} \text{ holds}\}$.

For splitting, we divide the interval $[0, L]$ into m sub-intervals with boundaries $0 = l_0 < l_1 < \dots < l_m = L$. Let the time of hitting the k -th level be $T_k = \inf\{t > 0 : \phi(\mathbf{X}(t)) \geq l_k\}$ and the event that the k -th level is hit during $[0, T]$ be $H_k = \{T_k < T\}$. Therefore, $\mathcal{P}(H_m) = \tilde{\gamma}$ and $\mathcal{P}(H_0) = 1$. As $H_m \subset H_{m-1} \subset \dots \subset H_1 \subset H_0$, we have, $\tilde{\gamma} = \mathcal{P}(R) = \prod_{k=1}^m \mathcal{P}(H_k|H_{k-1}) = \prod_{k=1}^m p_k$, where $p_k := \mathcal{P}(H_k|H_{k-1}) = \mathcal{P}(H_k)/\mathcal{P}(H_{k-1})$. Probability of hitting each of the k -th level, p_k , is estimated separately by generating independent sample paths from the distribution of the entrance state $G_{k-1} := (T_{k-1}, \mathbf{X}(T_{k-1}))$ conditioned on H_{k-1} at the threshold level l_{k-1} . The empirical distribution \hat{G}_k is an estimate of the entrance distribution G_k which is obtained from H_k . Thus we can proceed recursively, replacing \hat{G}_{k-1} for G_{k-1} and estimate p_k at each level k by the proportion of level hits, $\hat{p}_k = S_k/N_{k-1} \quad \forall S_k > 0$, with S_k are the number of sample paths where H_k occurs and N_k is the total number of sample paths at level k . $\hat{\gamma}$ is estimated by the product of \hat{p}_k 's: $\prod_{k=1}^m \hat{p}_k = \prod_{k=1}^m \frac{S_k}{N_{k-1}}$.

We use a variant of splitting called the Fixed Number of Successes (FNS) proposed by Amrein and Künsch (2011). For FNS the number of hits per level S_k is kept fixed. The process is independently repeated by selecting an entrance state at random and simulating the process from the selected state up to $\min\{T_k, T\}$ until S_k hits are observed. Using FNS one can avoid path extinction or explosion, however, computational effort is compromised. The unbiased estimator of the rare-event probability is given by

$$\hat{\gamma} := \prod_{k=1}^m \tilde{p}_k = \frac{S_k - 1}{N_{k-1} - 1}. \quad (8)$$

The unbiased estimator for the variance $\text{Var}(\hat{\gamma})$ is not known for the FNS method. However, under the assumption that the conditional hitting probability does not depend on the entrance states of the previous stage, $\mathcal{P}(H_k|H_{k-1}, (T_{k-1}, \mathbf{X}(T_{k-1}))) = \mathcal{P}(H_k|H_{k-1})$ for all $((T_{k-1}, \mathbf{X}(T_{k-1})), \forall k)$, the squared relative error of $\hat{\gamma}$ can be bounded :

$$\text{SRE}(\hat{\gamma}) \leq \prod_{k=1}^m \left(\frac{1}{S_k - 2} + 1 \right) - 1. \quad (9)$$

5.2 Importance Function for Calculating PLCV

The efficiency of splitting is significantly determined by the IF (Garvels, Van Ommeren, and Kroese 2002). We take the maximum of the ratio of the absolute value of line currents and their respective maximum line current capacity as the importance function $\phi(t)$. This makes $\phi(t)$ an increasing function in $[0,1]$ and it is given by

$$\phi(I_{i,j}(t)) := \max_{(i,j) \in \mathcal{E}} \frac{|I_{i,j}(t)|}{I_{i,j}^{\max}}. \quad (10)$$

At time t , for any $(i, j) \in \mathcal{E}$ if $|I_{i,j}(t)| \geq I_{i,j}^{\max}$ implies $\phi(I_{i,j}(t)) \geq 1$, signifying that the rare event is hit, i.e., one of the line currents has exceeded its line capacity. $\phi \rightarrow 1$ corresponds to approaching the rare event set. A similar IF was used by Wadman, Crommelin, and Frank (2013).

6 SIMULATION RESULTS

In this section we apply the SA algorithm and FNS to find the optimal storage position in a power network by minimizing PLCV.

6.1 Simulation Parameters

We first discuss the different parameters chosen for our simulations. For the O-U processes (2), we consider all the long term mean terms μ_i to be zero, which implies on an average at each non-slack node the power demand is compensated by the local power generation. The mean reverting terms $\theta_i = 1 + (i - 1)/(N - 2)$ for $i = 1, \dots, N - 1$ increases from 1 to 2 with i . The volatility terms σ_i are calculated from the long-term standard deviations of the O-U process $std(P_i(t)) = \sigma_i/\sqrt{2\theta_i}$. The values of $std(P_i(t))$ will be discussed in the subsequent sections. Currently, we only consider uncorrelated O-U processes for our assessment.

We perform our simulations for $T = 24$ hours and $\Delta t = 0.01$ hours. The initial state of the batteries are taken as $B_i(0) = B_i^{\max}/2 \forall i \in \mathcal{N}/\{1\}$, i.e, they are half-filled.

For performing FNS we first calculate the number of levels m by the pilot run such that \tilde{p}_k is nearly equal to the optimal value of $p_{\text{opt}} \approx 0.2032$ (Amrein and Künsch 2011). For the pilot run we use $R_k = 50$ for all k . For the final run we calculate R_k from (9) such that the $SRE(\hat{\gamma}) \leq 0.03$. In order to obtain an accurate estimate of the probabilities, FNS is repeated $n = 30$ times (suggested by Freund and Simon (1967)) to calculate the mean of the estimator, $\hat{\gamma}_n := \frac{1}{n} \sum_{i=1}^n \hat{\gamma}_i$. The squared relative error of the mean computed from the n samples is $SRE(\hat{\gamma}_n) := \frac{1}{n} SRE(\hat{\gamma}_i)$.

For SA we take initial temperature $T_c = 1$ and $\kappa = 0.99$. For the stopping criterion we take $n^{\max} = 1000, n_d = 300$ and $\varepsilon = 10^{-7}$.

6.2 IEEE-14 Bus Test Case

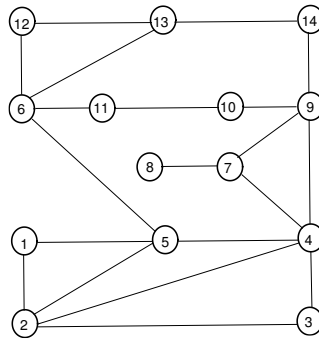


Figure 1: IEEE-14 bus line diagram showing the bus numbers and line connections. Bus 1 is the slack bus.

In Figure 1 the line diagram of the IEEE-14 bus test case is shown. We test our algorithm for different scenarios for the IEEE-14 bus test case. The different scenarios being different maximum current carrying capacity of the lines $I_{i,j}^{\max} \forall (i, j) \in \mathcal{E}$ and different standard deviations $std(P_i(t))$ of the O-U processes of the non-slack nodes and total installation capacity of storage B^{tot} . We use the MATPOWER package (Zimmerman, Murillo-Sánchez, and Thomas 2011) of MATLAB for the topological details (admittance matrix) of the IEEE-14 bus test case network. However, the maximum line current carrying capacity is not set by the test case. We will discuss the values of the maximum line current carrying capacities in the subsequent sections.

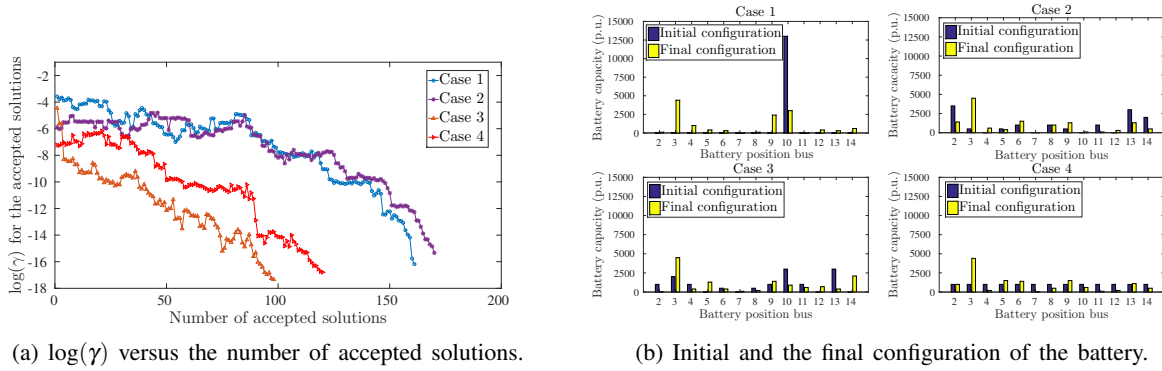


Figure 2: Figure 2a plots $\log(\gamma)$ versus the number of accepted solutions for different starting configuration of battery locations and capacities with $B^{\text{tot}} = 13000$ p.u. (Example 1). Figure 2b Compares the initial and the final configuration of the battery locations and capacities for four different initial states from Figure 2a.

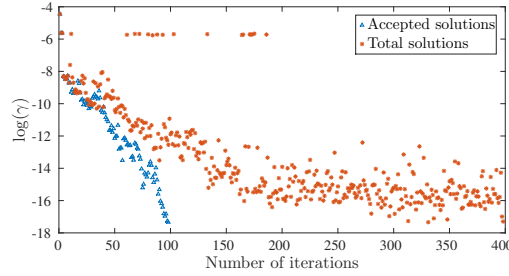


Figure 3: $\log(\gamma)$ versus the number of accepted solutions and total number to solutions the SA algorithm searched for (Case 3 of Example 1).

6.2.1 Example 1

For this case the values of $I_{i,j}^{\text{max}} \forall (i,j) \in \mathcal{E}$ were obtained by simulating a long time-series, $T=10^4$ hours, for the system. The maximum value of line currents attained from the time-series run was taken to be the allowed maximum of each lines. For the $\text{std}(P_i(t))$ we use the net power injections at each non-slack node from MATPOWER, the values range from 1 to 95 p.u. (where p.u. is per unit value of the quantity of interest).

We start from different random initial configurations (cases 1-4) of the battery locations and capacity to minimize $\log(\gamma)$. The total installation capacity of storage $B^{\text{tot}} = 13000$ p.u. For the random movement of the algorithm in the battery configuration space (section 4.2) we take the battery unit $\Delta B = 100$ p.u., the initial number of blocks exchanged $N_B = 5$ and $\Delta m = 1$.

From Figure 2a we observe that γ has reduced by roughly a factor of e^{10} . In Figure 2b we compare the initial and final configurations of the battery position and capacities. It is observed that for all the cases in the final configurations about 35 percent of B^{tot} is placed at bus 3. One plausible reason for this final configuration can be the fact that $\frac{\text{std}(P_3(t))}{\sum_{i=2}^{14} \text{std}(P_i(t))} = 0.365$. We note that the final battery sizes at all the other nodes (apart from 3) are different for all the four cases and are not as consistent as node 3. Notwithstanding, for all four cases γ is reduced to very small values, see Figure 2a.

In Figure 3 we compare the accepted configuration solutions with the total configuration solutions the algorithm has searched for (from case 3).

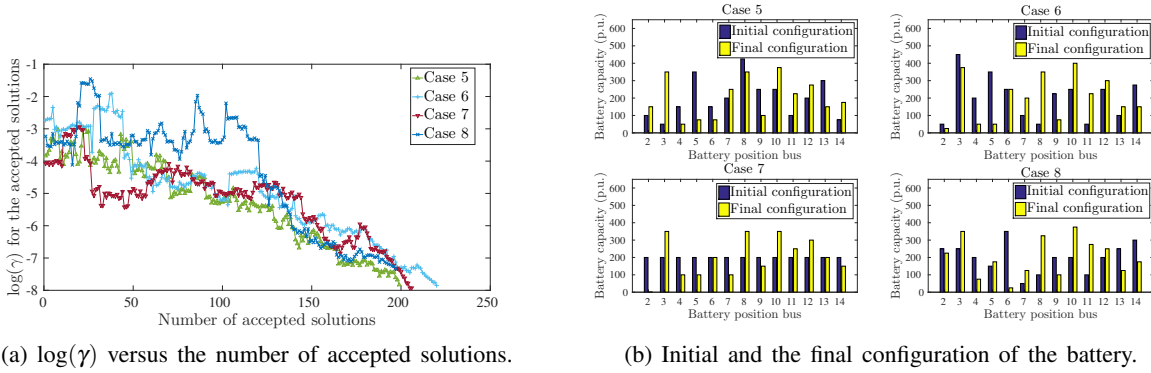


Figure 4: Figure 4a plots $\log(\gamma)$ versus the number of accepted solutions for different starting configuration of battery locations and capacities with $B^{\text{tot}} = 2600$ p.u. (Example 2). Figure 4b Compares the initial and the final configuration of the battery locations and capacities for four different initial states from Figure 4a.

6.2.2 Example 2

In this example, we take all the non-slack nodes to be similar, i.e., all the OU processes have same standard deviations $\text{std}(P_i(t)) = 10$ p.u. $\forall i \in \mathcal{N} \setminus \{1\}$. Unlike Example 1 we randomize the $I_{i,j}^{\text{max}}$. To do this, we perform a long time series run, $T=10^4$ hours, for the system to calculate the maximum current flown through each lines, and multiply them with uniform random numbers between $[0.5, 1]$ to obtain $I_{i,j}^{\text{max}}$. We take the battery unit $\Delta B = 12.5$ p.u., the initial number of blocks exchanged $N_B = 8$ and $\Delta m = m_B/2$ (section 4.2).

Figure 4a shows the minimization of $\log(\gamma)$ for four different initial configurations. We find that γ is reduced by a factor of e^4 . By comparing the initial and final configurations of the battery locations in Figure 4b, we find that buses 3, 8 and 10 require each around 15 percent of B^{tot} for all the cases for this minimization.

6.2.3 Example 3

In the example we make all the non-slack nodes and connection lines equivalent to study the effect of number of connections at nodes on the optimization. To do so, we take $\text{std}(P_i(t)) = 10$ p.u. $\forall i \in \mathcal{N} \setminus \{1\}$ and $I_{i,j}^{\text{max}} = 50$ p.u. $\forall (i, j) \in \mathcal{E}$. We take the battery unit $\Delta B = 12.5$ p.u., the initial number of blocks exchanged $N_B = 8$ and $\Delta m = m_B/2$ (section 4.2). Figure 5a shows the optimization of $\log(\gamma)$ for various cases, where each case represents a different starting configuration. The initial and final configurations of the battery placement is shown in Figure 5b. Notice for Case 11 when the batteries are placed equally at the non-slack buses the SA algorithm is not able to minimize $\log(\gamma)$ further. This hints towards the fact that equally placing the batteries at the non-slack buses is near optimal solution to the problem. Equal battery placement being the near optimal solution shows that number of connections at nodes is not important for minimizing $\log(\gamma)$.

We now investigate how $\log(\gamma)$ varies with B^{tot} . In order to do that we place the batteries equally at the non-slack buses. We do this because, Figure 5a suggests that equally placing the batteries at the non-slack buses is near the optimal solution of the problem. Figure 6 shows a linear relation between $\log(\gamma)$ and B^{tot} .

Finally we study the effect of B^{tot} on the final configuration of battery locations and capacities. We compare the final configurations for $B^{\text{tot}} = 1300$ p.u. and 2600 p.u. For both the cases we start from equally placing the batteries at the non-slack buses and start the optimization from a lower temperature $T_c = 0.05$. We do this because equal battery placement is already near the optimal solution. We repeat the optimization 10 times for different B^{tot} and take an average for presenting the final configurations in

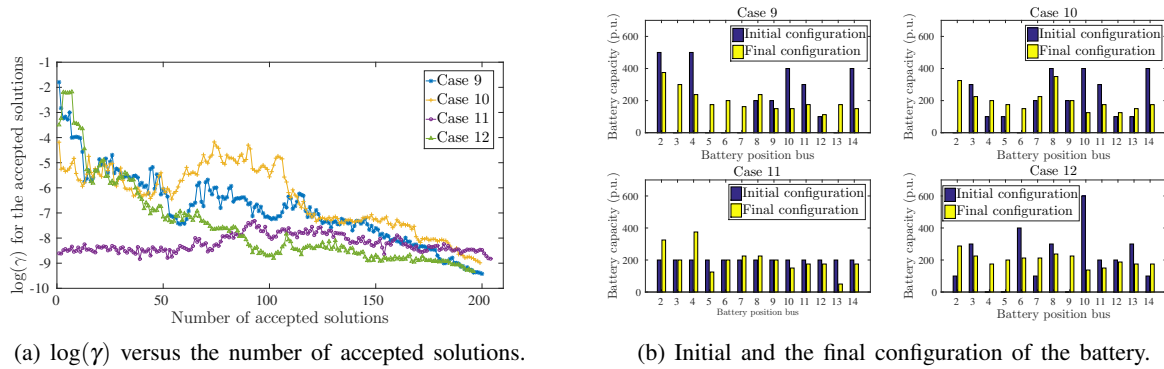


Figure 5: Figure 5a plots $\log(\gamma)$ versus the number of accepted solutions for different starting configuration of battery locations and capacities with $B^{\text{tot}} = 2600$ p.u. (Example 3). Figure 5b Compares the initial and the final configuration of the battery locations and capacities for four different initial states from Figure 5a.

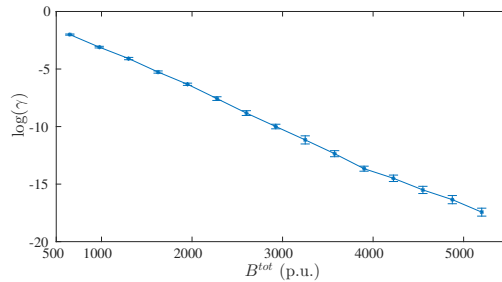


Figure 6: $\log(\gamma)$ versus B^{tot} . The error bars represents 95 percent confidence interval of $\log(\gamma)$.

Figure 7. Doubling B^{tot} does not affect the final configuration of the batteries, it almost doubles the size of batteries at the final configuration as shown in Figure 7.

7 CONCLUSIONS

For finding the optimal storage placement to enhance power network reliability we use a novel combination of two computational techniques namely Simulated Annealing and the Splitting technique for rare-event simulation. To best of our knowledge this combination has not been used before. We use simulated annealing to minimize the reliability index, PLCV (γ), of the network. We find that for very small values of γ , SA might not converge, however this problem disappears if we use $\log(\gamma)$ instead of γ as the cost function in SA. In order to calculate the small values of γ 's we use FNS splitting technique for rare-event simulation.

We apply our method to the IEEE-14 bus network for three different examples. In example 1 we have different nodal power injections and line current maxima. For this example we find that at the final configuration (after the minimization), bus 3 has 35 percent of B^{tot} . In example 2 we keep the nodal power injections to be similar and find that at the final configuration buses 3, 8 and 10 each get 15 percent of B^{tot} .

For example 3 we keep all the nodal power injections and the line current maxima to be similar. For this we find that equal placement of the batteries at the non-slack nodes is the near optimal solution, which suggests that the number of connections to a node does affect the reliability of the power network. We also find that the $\log(\gamma)$ decreases linearly with B^{tot} . Finally we examine if B^{tot} has an effect on final configuration of the battery locations and capacities. We observe that it does not affect the final configuration.

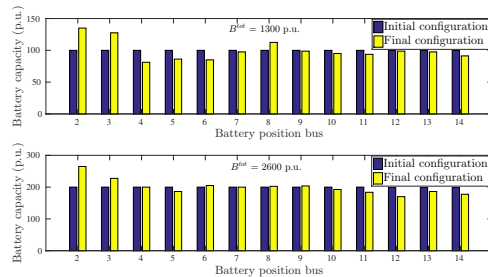


Figure 7: Comparing the initial and the final configuration of the battery locations and capacities for $B^{\text{tot}} = 1300$ p.u. and 2600 p.u.

ACKNOWLEDGMENTS

This work is a part of the Industrial Partnership Program (IPP) ‘Computational sciences for energy research’ of the Foundation for Fundamental Research on Matter (FOM), which is financially supported by the Netherlands Organization for Research (NWO). This research program is co-financed by Shell Global Solutions International B.V.

REFERENCES

- Aburub, H., and W. T. Jewell. 2014. “Optimal Generation Planning to Improve Storage Cost and System Conditions”. In *2014 IEEE Power and Energy Society General Meeting— Conference & Exposition*, 1–5. Piscataway, New Jersey: Institute of Electrical and Electronics Engineers, Inc.
- Amrein, M., and H. R. Künsch. 2011. “A Variant of Importance Splitting for Rare Event Estimation: Fixed Number of Successes”. *ACM Transactions on Modeling and Computer Simulation* 21 (2): 13.
- Barton, J. P., and D. G. Infield. 2004. “Energy Storage and its use with Intermittent Renewable Energy”. *IEEE Transactions on Energy Conversion* 19 (2): 441–448.
- Bhaumik, D., D. T. Crommelin, and B. Zwart. 2015. “Mitigation of Large Power spills by a Storage Device”. Submitted, <http://persistent-identifier.org/?identifier=urn:nbn:nl:ui:18-23525>.
- Bose, S., D. F. Gayme, U. Topcu, and K. M. Chandy. 2012. “Optimal Placement of Energy Storage in the Grid”. In *IEEE 51st Annual Conference on Decision and Control (CDC)*, 5605–5612. Piscataway, New Jersey: Institute of Electrical and Electronics Engineers, Inc.
- Chandy, K. M., S. H. Low, U. Topcu, and H. Xu. 2010. “A Simple Optimal Power Flow Model with Energy Storage”. In *49th IEEE Conference on Decision and Control (CDC)*, 1051–1057. Piscataway, New Jersey: Institute of Electrical and Electronics Engineers, Inc.
- Freund, J. E., and G. A. Simon. 1967. *Modern Elementary Statistics*, Volume 256. Prentice-Hall Englewood Cliffs, New Jersey.
- Garvels, M. 2000. *The Splitting Method in Rare Event Simulation*. Ph. D. thesis, Universiteit Twente.
- Garvels, M. J., J.-K. C. Van Ommeren, and D. P. Kroese. 2002. “On the Importance Function in Splitting Simulation”. *European Transactions on Telecommunications* 13 (4): 363–371.
- Gayme, D., and U. Topcu. 2013. “Optimal Power Flow with Large-Scale Storage Integration”. *IEEE Transactions on Power Systems* 28 (2): 709–717.
- Ghofrani, M., A. Arabali, M. Etezadi-Amoli, and M. S. Fadali. 2013. “A Framework for Optimal Placement of Energy Storage Units within a Power System with High Wind Penetration”. *IEEE Transactions on Sustainable Energy* 4 (2): 434–442.
- Grainger, J. J., and W. D. Stevenson. 1994. *Power System Analysis*, Volume 31. McGraw-Hill New York.
- Oh, H. 2011. “Optimal Planning to Include Storage Devices in Power Systems”. *IEEE Transactions on Power Systems* 26 (3): 1118–1128.
- Rubino, G., B. Tuffin et al. 2009. *Rare Event Simulation using Monte Carlo Methods*. Wiley Online Library.

- Shortle, J., S. Rebennack, and F. W. Glover. 2014. “Transmission-Capacity Expansion for Minimizing Blackout Probabilities”. *IEEE Transactions on Power Systems* 29 (1): 43–52.
- Sjödin, E., D. F. Gayme, and U. Topcu. 2012. “Risk-Mitigated Optimal Power Flow for Wind Powered Grids”. In *2012 American Control Conference (ACC)*, 4431–4437. Piscataway, New Jersey: Institute of Electrical and Electronics Engineers, Inc.
- van den Akker, J., S. Leemhuis, and G. Bloemhof. 2014. “Optimizing Storage Placement in Electricity Distribution Networks”. In *Operations Research Proceedings 2012*, 183–188. Springer.
- Van Laarhoven, P. J., and E. H. Aarts. 1987. *Simulated Annealing: Theory and Applications*, Volume 37. Springer Science & Business Media.
- Varaiya, P. P., F. F. Wu, and J. W. Bialek. 2011. “Smart Operation of Smart Grid: Risk-Limiting Dispatch”. *Proceedings of the IEEE* 99 (1): 40–57.
- Wadman, W., D. Crommelin, and J. Frank. 2013. “Applying a Splitting Technique to Estimate Electrical Grid Reliability”. In *Proceedings of the 2013 Winter Simulation Conference: Simulation: Making Decisions in a Complex World*, 577–588. Piscataway, New Jersey: Institute of Electrical and Electronics Engineers, Inc.
- Wadman, W. S., D. T. Crommelin, and B. P. Zwart. 2016. “A Large-Deviation-Based Splitting Estimation of Power Flow Reliability”. *ACM Transactions on Modeling and Computer Simulation (TOMACS)* 26 (4): 23.
- Yau, T., L. N. Walker, H. L. Graham, A. Gupta, and R. Raithel. 1981. “Effects of Battery Storage Devices on Power System Dispatch”. *IEEE Transactions on Power Apparatus and Systems* (1): 375–383.
- Zimmerman, R. D., C. E. Murillo-Sánchez, and R. J. Thomas. 2011. “MATPOWER: Steady-State Operations, Planning, and Analysis Tools for Power Systems Research and Education”. *IEEE Transactions on Power Systems* 26 (1): 12–19.

AUTHOR BIOGRAPHIES

DEBARATI BHAUMIK is a PhD student in the Scientific Computing group at CWI Amsterdam. She received her M.Sc. degree in Physics from IIT Madras, India in 2012. Her PhD topic is reliability and robustness of power grids with uncertain generations, and her present research interests include stochastic modelling, integration of renewables in power network and Monte Carlo techniques for rare-event simulation. Her email address is bhaumik@cwi.nl.

DAAN CROMMELIN leads the Scientific Computing group at CWI Amsterdam and holds a position as professor of Numerical Analysis and Dynamical Systems at the University of Amsterdam. He received his PhD from Utrecht University in 2003 and worked as a postdoc at New York University’s Courant Institute before joining CWI. His research focuses on stochastic and computational methods for multiscale dynamical systems, with applications in atmosphere-ocean science and energy systems. His email address is Daan.Crommelin@cwi.nl.

BERT ZWART is a researcher at the Center for Mathematics and Computer Science (CWI) in Amsterdam, where he leads the Stochastic group. He also holds a professorial positions at Eindhoven University of Technology. His research is in applied probability, inspired by problems in computer, communication, energy and service networks. Zwart is the 2008 recipient of the Erlang prize, an IBM faculty award, VENI, VIDI and VICI awards from the Dutch Science Foundation NWO, the 2015 Van Dantzig Prize, and 4 best papers awards. His email address is Bert.Zwart@cwi.nl.